

Attitude Control on TET-1 and BIROS - Experiences from the FireBird Mission and End of Life Operations

Lukas Hoffmann^{a*}, Thomas Terzibaschian^b, Dr. Katrin Wirth^c, Jens Hartung^d, Arvind Kumar Balan^e

^a *Deutsches Zentrum für Luft- und Raumfahrt e. V., German Aerospace Center, Germany, l.hoffmann@dlr.de*

^b *Deutsches Zentrum für Luft- und Raumfahrt e. V., Institute of Optical Sensor Systems, Germany,
Thomas.Terzibaschian@dlr.de*

^c *Deutsches Zentrum für Luft- und Raumfahrt e. V., German Aerospace Center, Germany, katrin.wirth@dlr.de*

^d *Deutsches Zentrum für Luft- und Raumfahrt e. V., German Aerospace Center, Germany, jens.hartung@dlr.de*

^e *Deutsches Zentrum für Luft- und Raumfahrt e. V., German Aerospace Center, Germany, arvind.balan@dlr.de*

* Corresponding Author

Abstract

The satellite TET-1 (Technologie-Erprobungsträger 1) was launched in 2012 as part of the DLR On-Orbit-Verification program (OOV). Together with the second satellite BIROS (Bi-spectral InfraRed Optical System), which was launched in 2016, they represented the space segment of the scientific FireBird mission. The primary goal of the mission was to perform Earth observations in the infrared spectrum for high-energy events such as forest fires and to contribute valuable data to the scientific community and the International Charter on Space and Major Disasters. After seven years of successful operations, the FireBird project ended in December 2020. Both satellites are now monitored and operated by a significantly reduced operations team until their re-entry into the Earth's atmosphere.

The AOCS subsystem, like the satellite as a whole in project Phase E, has only two physical interfaces to the ground segment: telemetry and telecommands. Safety, reliability and efficiency in ongoing mission operations depend on these two interfaces. It must be assured at all times that the AOCS subsystem can be safely transitioned from one defined state to another. This paper shows on selected examples of TET-1 and BIROS, different aspects of the performance of the attitude control system as well as the operational challenges over the years in Phase E. The long-term impact of a permanent reaction wheel failure which occurred at an early stage of the TET-1 mission is discussed. In order to estimate the general degradation of the AOCS units, the amount and distribution of autonomous unit power cycles as part of the FDIR system with respect to the geographical location, space weather and operational as well as non-operational uptime is analyzed. Following this, the interdependency between the orbit and the operational temperature of the star tracker heads with respect to the amount of valid measurements is outlined. The operational effects and limitations due to the loss of the main Inertial Measurement Unit in 2019 as well as the degradation of the backup unit is described and the resulting consequences are discussed. Finally, the performance of the GPS receivers and the long-term degradation is shown based on the ability to provide a valid solution. In a subsequent section, the flyby and communication experiments performed in 2019 and 2020 between BIROS and the pico-satellite BEESAT-4 are described and the commanding approach for achieving the pointing accuracy and results are presented. In the final section, a brief conclusion and outlook for the remaining years are given.

Keywords: FireBird, Satellite Operations, AOCS

Acronyms/Abbreviations

Auto Acquisition Mode (AAM)
Attitude and Orbit Control System (AOCS)
Berlin Experimental and Educational Satellite 4 (BEESAT-4)
Bi-spectral InfraRed Optical System (BIROS)
Bi-spectral and Infrared Remote Detection (BIRD)
Coarse Sun Sensor (CSS)
Client Orientation Mode (COM)
Deutsches Zentrum für Luft- und Raumfahrt (DLR) – German Aerospace Center
End-of-Life (EOL)
Earth Pointing Mode (EPM)
Fault Detection, Isolation and Recovery (FDIR)
German Space Operations Center (GSOC)
Global Positioning System (GPS)

High Torque Wheels (HTW)
Inertial Measurement Unit (IMU)
Inertial Pointing Mode (IPM)
Local Time of Ascending Node (LTAN)
Magnetic Coil System (MCS)
Magnetic Field Sensor (MFS)
National Oceanic and Atmospheric Administration (NOAA)
On-board Navigation System (ONS)
Polar Satellite Launch Vehicle (PSLV)
Reaction Wheel (RW)
Safe Mode (SFM)
Advanced Stellar Compass (ASC)
Sun Pointing Fix Mode (SPFM)
Sun Pointing Rotate Mode (SPRM)
Technologie-Erprobungsträger 1 (TET-1)
Thruster Firing Mode (TFM)
Thruster Unit (THR)
True of Date (TOD)
Ultra-High-Frequency (UHF)

1. Introduction

The satellite platform for TET-1 and BIROS was developed as a cost-effective solution for the verification of new technologies in space based on the satellite BIRD (Bi-spectral and Infrared Remote Detection) which was launched in 2001 and operated successfully for several years [1]. The manufacturing of the two satellites was done by the Kayser-Threde GmbH and Astro- und Feinwerktechnik Adlershof GmbH in cooperation with DLR. TET-1 was launched in 2012 from Baikonur with a Soyuz rocket and initially part of the DLR On-Orbit-Verification program (OOV) for the demonstration and qualification of new spacecraft technology until the FireBird mission started in November 2013 [2]. In 2016, BIROS was launched from the Satish Dhawan Space Center in India with a PSLV and joined TET-1 in the mission. Both satellites were inserted into polar orbits with an altitude between 480 and 510 km and an inclination of $\sim 97.5^\circ$. Over the years, the two satellites successfully performed Earth observations in the infrared spectrum for high energy events such as forest fires but also supported studies related to low temperature environments like the surface of the sea. Compared to other fire detecting satellite missions, TET-1 and BIROS were able to take images with a higher spatial resolution and perform more accurate measurements of fire intensities [3]. Spacecraft operations during the LEOP, Phase E and the End-of-Life (EOL) phase was and still is conducted at the German Space Operations Center (GSOC) of DLR.

After 7 years of operations, TET-1 was withdrawn from the FireBird mission in October 2019 due to a non-recoverable failure of the payload support system related power converter which prevented the further usage of the camera system. Since the satellite bus was still functioning, an EOL strategy was developed to perform regular monitoring and data collection. The number of contacts was reduced from four per day to four per week. This was determined to be the minimum number required to ensure the downlink of all offline recorded on-board data with the lowest supported S-band downlink rate of 137 kbit. It also allowed a close monitoring of the orbit in case of satellite collision warnings. Data gaps were reduced to a minimum and tolerated during contingency situations such like satellite Safe Modes or in case of problems with the ground segment. The overall achieved availability of TET-1 data after the entry in the EOL phase was 97.4% compared to 95.4% during the mission. All remaining contacts were performed with a low priority at the Weilheim groundstation which belongs to the same DLR institute as GSOC. On ground segment level, an automation tool was developed at GSOC to take over the routine commanding tasks as well as the basic S/C status monitoring. TET-1 re-entered the Earth's atmosphere during the night between 18th and 19th of November 2022, approximately one day after the last successful contact was performed.

The FireBird mission was continued for more than one year with BIROS as single satellite until 2020, when it transitioned into an EOL operations phase as well. The EOL concept of BIROS was set up similar to TET-1 with a data availability of 97.9% after the entry to the EOL phase, compared to 99.1% during the FireBird mission. BIROS now serves as platform for operational experiments in cooperation with other DLR institutes and universities and is further used for the training of GSOC personnel.

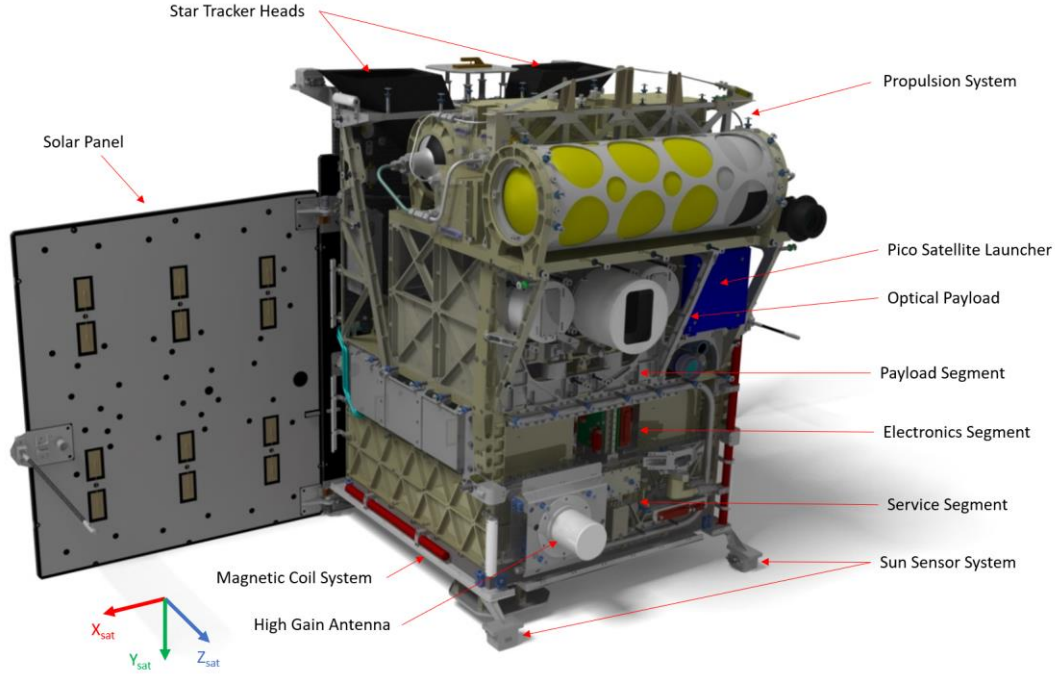


Fig. 1. Overview of the BIROS satellite with the description of visible components [4]

2. The Attitude and Orbit Control System of TET-1 and BIROS

The AOCS of TET-1 and BIROS provides a three-axis stabilized attitude and consists of several sensors for attitude determination as well as actuators for attitude control. By design, a single failure tolerance was achieved using hardware units in hot and cold redundancy as listed in Table 1. One feature of the AOCS is the On-board Navigation System (ONS) which uses data from the GPS receiver to calculate the inertial orientation of the Earth as well as the direction of the Sun vector and the magnetic field vector based on an International Geomagnetic Reference Field model. In case no GPS data is available, the ONS uses a prediction algorithm to calculate the current position of the satellite. In contrast to TET-1, BIROS is additionally equipped with an experimental nitrogen based resistojet propulsion system and a set of three experimental High Torque Wheels [5].

Table 1. Sensors and Actuators used by the AOCS of TET and BIROS. The redundancy configuration describes the actively used and total available units during a Fine Pointing Mode.

	Redundancy Configuration
Sensors	
Coarse Sun Sensor (CSS)	Hot (2/2)
Magnetic Field Sensor (MFS)	Cold (1/2)
Inertial Measurement Unit (IMU)	Cold (1/2)
Advanced Stellar Compass - Star Tracker System (ASC)	Cold (1/2)
Global Positioning System (GPS)	Cold (1/2)
Actuators	
Magnetic Coil System (MCS)	Cold (1/2)
Reaction Wheels (RW)	Hot (4/4)
High Torque Wheels (HTW) only BIROS	Experiment (3/3)
Thruster Unit (THR) only BIROS	Experiment (1/2)

In order to fulfil all requirements given by the experiments, different attitude modes are implemented in the AOCS on-board S/W. The modes can be divided into one-axis stabilized Coarse Pointing Modes and three-axis stabilized Fine Pointing Modes. The Coarse Pointing Modes are mainly used during and after a satellite Safe Mode or in case a Fine Pointing Mode cannot be established. This can be the case if required sensor input is missing or if actuators are not available. During routine operations, the Sun Pointing Fix Mode (SPFM) and Earth Pointing Mode

(EPM) are used primarily. The SPFM points the -z axis towards the Sun to maximize the power generated by the solar panels. The +x-axis is thereby aligned to the inertial north. The EPM points the +z axis nadir to Earth to support image acquisitions with the optical payload as well as data downlinks via the High Gain Antenna. The orientation of the satellite axes can be seen in Fig. 1. In order to provide the precise orientation for payload operations, the Fine Pointing Modes have an accuracy of below 5 arcmin. The Suspend Mode is used as transition mode where no attitude control is performed while the entry conditions for the commanded mode are verified. An overview of all available AOCS modes is shown in Table 2 [6].

Table 2. Overview of all AOCS modes, the pointing targets and the used sensors and actuators. The TFM, FSM and COM are only available on BIROS.

AOCS Mode	Pointing Target	Used Sensors	Used Actuators
Suspend Mode (SPM)	No pointing (transition mode)	Same as previous mode	None
Coarse Pointing Modes			
Safe Mode (SFM)	Coarse Sun pointing for solar panels	CSS, MFS,	MCS,
Auto Acquisition Mode (AAM)	Satellite rate reduction and Sun pointing	IMU, ONS	RWs
Fine Pointing Modes			
Earth Pointing Mode (EPM)	Pointing +z Nadir		
Sun Pointing Fix Mode (SPFM)	Pointing -z to Sun		
Sun Pointing Rotation Mode (SPRM)	Pointing -z to Sun with rotation around the Sun vector	CSS, MFS, IMU, ASC,	MCS, RWs
Target Pointing Mode (TPM)	Pointing to +z to WGS84 target coordinates	ONS, GPS	
Inertial Pointing Mode (IPM)	Pointing according to target quaternions		
Thruster Firing Mode (TFM)	Alignment of thrusters for orbit maneuver		
Fast Slew Mode (FSM)	Experimental Mode for payload operations		
Client Orientation Mode (COM)	Experimental Mode for payload operations		

The distribution of used AOCS modes can be seen in Table 3. TET-1 and BIROS achieved a total time in Fine Pointing Modes during Phase E of 95.9 % and 98.1%, respectively. As mentioned above, the most commonly used mode was the SPFM, pointing the solar panel towards the Sun. The Sun Pointing Rotation Mode (SPRM) was temporarily used as standard Sun pointing mode in the beginning of the mission of TET-1 to increase the heat radiation until the RW1 failure occurred. The EPM was used for roughly 5% of the total time. When TET-1 left the FireBird mission after seven years and entered the EOL phase, the percentage of Coarse Pointing Mode increased significantly. In March 2022, based on the rising degradation of hardware units in combination with the limited support of operations engineers, it was decided to use the Auto Acquisition Mode (AAM) as main AOCS mode for the nominal Sun pointing attitude instead of the SPFM. This reduced the number of autonomous mode transitions between SPFM and AAM when the required sensor information for establishing a Fine Pointing Mode was temporarily missing. When BIROS transitioned into the EOL phase, the distribution of AOCS modes remained similar to the Phase E. This can be explained by the younger age of the satellite. The main Sun pointing attitude was and still is the SPFM. Due to end of the payload operations and the reduced number of uplink contacts, the percentage of time using the EPM decreased from 5 % down to 1.8%.

Table 3. Percentage of AOCS modes used during Phase E and after the transition to EOL operations.

AOCS Mode [%]	TET-1	TET-1	BIROS	BIROS
	Phase E	End-of-Life	Phase E	End-of-Life
	2012-2019	2019-2022	2016-2020	2020-2022
Suspend Mode (SPM)	<0.1	0.8	0.2	0.2
Coarse Pointing Modes				
Safe Mode (SFM)	4.0	23.8	1.6	2.0
AutoAcquisition Mode (AAM)	0.5	0.4	0.2	0.2
	3.5	23.4	1.3	1.8

Fine Pointing Modes	95.9	75.4	98.1	97.8
Earth Pointing Mode (EPM)	5.4	<0.1	5.0	1.8
Sun Pointing Fix Mode (SPFM)	85.6	75.4	90.4	96.0
Sun Pointing Rotation Mode (SPRM)	4.9	0	<0.1	0
Target Pointing Mode (TPM)	<0.1	0	0.2	<0.1
Inertial Pointing Mode (IPM)	<0.1	0	<0.1	<0.1
Thruster Firing Mode (TFM)			0.1	<0.1
Fast Slew Mode (FSM)			<0.1	0
Client Orientation Mode (COM)			2.1	0

3. Failure of both Inertial Measurement Units on TET-1

The Inertial Measurement Units are used as primary input for the determination of the satellite rotation rates. In case no IMU is available or if the AOCS rejects the measurements, the rotation rates are calculated based on star tracker data. This alternative method represents no reduction of the AOCS functionality. In case no star tracker data is available due to blinding effects by the Sun, Earth or Moon, or if the star tracker system is switched off during contingency situations, the AOCS calculates the satellite rates using the Sun and magnetic field sensors in combination with the ONS. This leads to a reduction in precision and can be done only when a Sun reference is available. During eclipse phases, the satellite rate is solely computed using the magnetic field sensors. This provides limited information for the attitude determination and is not sufficient for most payload operations.

In February 2019, an abrupt loss of communication between the active IMU-1 and the TET-1 bus occurred. The on-board AOCS surveillance application triggered an autonomous power-cycle of the unit which had no effect. The unavailability of an active IMU-1 then caused attitude instabilities during periods where the star trackers were blinded. Three hours after the failure and with a reduced pointing accuracy of the solar panel, the on-board computer triggered a satellite Safe Mode due to a battery undervoltage. Further tests with IMU-1 were performed in the following days without success. IMU-1 was declared faulty 2390 days after launch and after 1442 days of active operation. It was consequentially disabled for the AOCS and locked in a powerless state to prevent further usage and communication to this sensor unit. A modification of the on-board FDIR mechanisms was performed to ensure the usage of the cold redundant IMU-2 for the estimation of the satellite rotations. During the following utilization of IMU-2, no performance difference was detected compared to IMU-1 but an increasing number of autonomous power-cycles was observed as described in section five. Further analysis showed a rising noise level in the measured rotation rates. This led to temporary periods without active IMU due to a too high number of exceeded rate errors. Two comparable time periods showing the measured satellite rates by the IMUs in 2013 and 2022 are shown in Fig. 2. It can be seen that measurements in 2022 contained a high level of noise with spikes above 0.4 deg/s. Satellite rates measured by IMU-1 in 2013 as well as by the star trackers, due to a downtime of the IMU, showed a significantly lower level of calculated satellite rates.

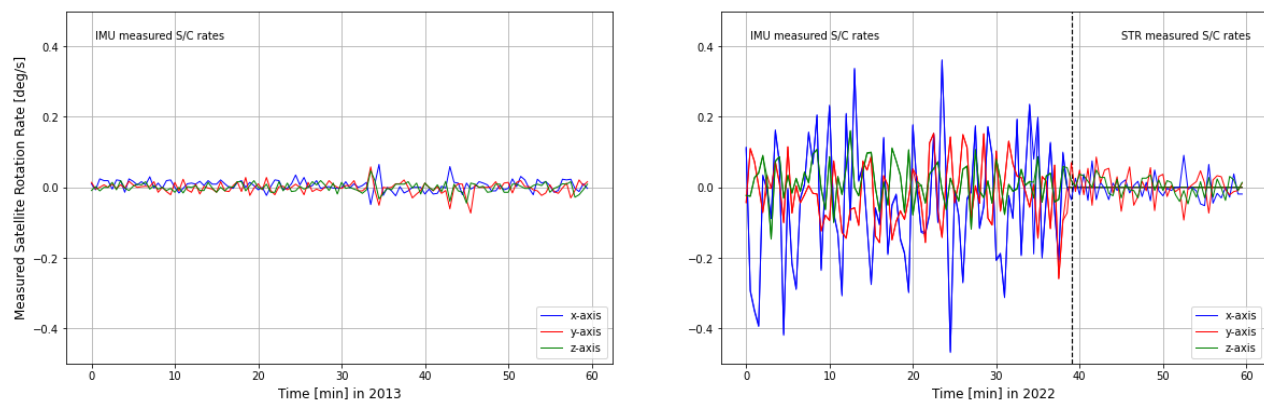


Fig. 2. 60 minutes of measured satellite rates in 2013 and 2022. The measured satellite rates in the left plot are based on IMU-1, whereas the satellite rates in the right plot are based on the IMU-2 and the STR.

The number of exceeded rate errors and related downtimes of IMU-2 further increased until June 2022 where IMU-2 measurements were permanently unavailable and a satellite Safe Mode was initiated due to battery undervoltage situation. This occurred 3626 days after launch and after 2153 days of active operation. In contrast to

the failure of IMU-1 and because of short reoccurring periods of active measurements, IMU-2 was kept enabled in the AOCS loop and no major changes of the FDIR mechanisms were performed.

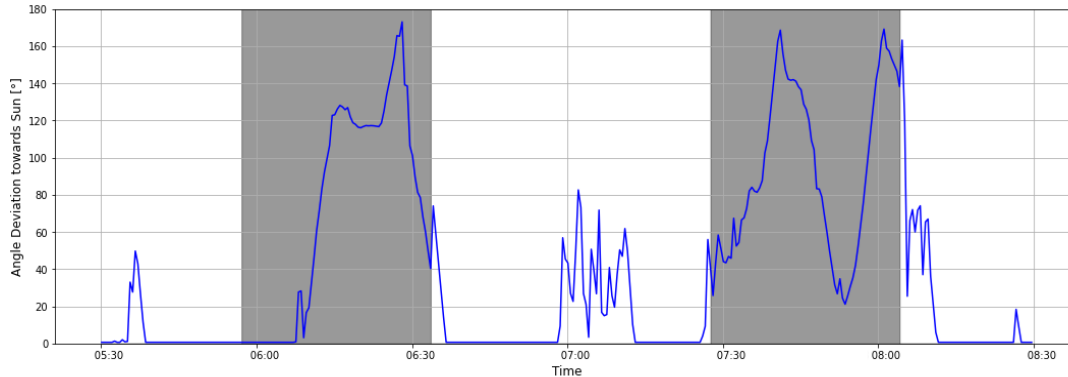


Fig. 3. Exemplary time frame in 2022 without IMU measurements showing the angular deviation between the direction of the Sun and the solar panel. Grey areas indicate eclipse phases.

Follow-up analysis on the AOCS behaviour in SPFM and AAM without permanent active IMU measurements revealed a sufficient functionality to establish a Sun pointing attitude. The overall maximum pointing deviation between the solar panels and the Sun direction was calculated to be 26° . In Sun phases where a combination of STR, CSS, MFS and ONS were used, the maximum deviation was calculated to be 15° whereas this error increased to 42° in eclipse phases. Fig. 3 shows the angle deviation between solar panel and Sun direction during an exemplary time frame in 2022 without the measurements of the satellite rates by an active IMU. As one consequence of an overall higher attitude deviation, the maximum allowed charge of the battery was increased to compensate the reduced solar panel output.

4. Reaction Wheel Failure and comparison between three-wheel and four-wheel configuration

As described in section 2, the AOCS of TET-1 and BIROS primarily use reaction wheels for attitude control. Due to external torques, such as gravity gradient torque or solar radiation pressure torque, a desaturation of the reaction wheels by using magnetorquers is required [7]. The four reaction wheels were mounted in a tetrahedral configuration in the service segment of the satellite bus. Compared to an orthogonal configuration with three reaction wheels, a higher torque and momentum storage capability can be achieved. A further advantage is a one failure redundancy and the distribution of angular momentum to all four reaction wheels during slews in the satellite axes [8]. As seen by the missions Kepler [9], Dawn [10] and others, reaction wheels can be counted among the more complex hardware units of the AOCS and have a higher risk of failures compared to magnetorquers or other units which consist of no mechanically moving parts.

In February 2013, a satellite Safe Mode was triggered on TET-1 due to a temporary failure of the primary IMU while in SPRM. This led to a high load on the reaction wheels and tripped the temperature dependent fuse on RW1 which is used to isolate short circuits in the reaction wheel electronics. After several attempts to recover the reaction wheel, an additional error in the EEPROM of RW1 occurred. This resulted in a higher power delivery and caused an irreversible damage and loss of the reaction wheel. Due to the limited telemetry available during this timeframe, no further failure analysis was possible and after the execution of several tests, RW1 was declared as faulty. As with the failure of IMU-1 described in section three, a modification of the FDIR mechanisms was performed to assure the isolation of the reaction wheel.

The mission was continued for another six years with a three-wheel configuration without noticeable decrease in the performance of the TET-1 AOCS. To evaluate this, the capability to perform attitude slews was analysed and compared to the four-wheel configuration of BIROS. In Fig. 4, the slew times with respect to the slew angles for TET-1 and BIROS after two years into the mission are shown. It can be seen that both satellites were able to achieve slew rates close to the target slew rate of $0.5^\circ/\text{s}$ and therefore fulfilled the design goal with only few exceptions. Not considered in the plots of Fig. 4 is the time for satellite acceleration and deceleration which is performed with $0.1^\circ/\text{s}^2$. The unequal distribution of slew angles between both satellites is related to the different orbit characteristics, mainly the beta angle, causing a variation in the angle between a Sun pointing attitude and an Earth pointing attitude. A more detailed analysis of slew times is limited by the low sampling rate of available offline data.

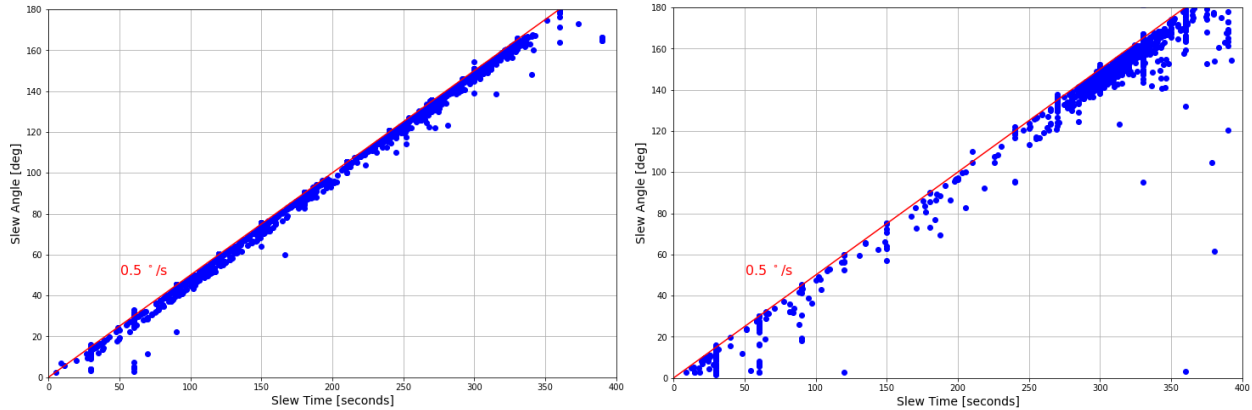


Fig. 4. Dependency between observed slew times and slew angles after two years in space. The red line shows the designed target satellite rotation rate of 0.5 °/s. Left: TET-1 attitude slews in 2014. Right: BIROS attitude slews in 2018.

Per design, the failure of a second reaction wheel on TET-1 resulted in the transition to AOCS Safe Mode (SFM). In order to stabilize the satellite, the spin rate of the two remaining reaction wheels was kept constant and the magnetorquers were used to establish a one-axis stabilized Sun pointing attitude. This happened once in 2018 and once in 2019 when reaction wheel 3 temporarily stopped working after a satellite Safe Mode. Due to the limited capabilities of the magnetorquers and the limitation that a torque can only be generated perpendicular to the Earth's magnetic field, no precise and predictable pointing was possible in this configuration until a recovery of the failed RW 3 was performed. A permanent failure of a second reaction wheel would have significantly limited further payload operations.

5. Autonomous AOCS Unit Power-Cycles

During an update of the TET-1 bus software in August 2013, the autonomous power-cycling of AOCS units was introduced. This function is performed by the AOCS surveillance application and is triggered, in case the IMU does not deliver data for over 10 control cycles, a Reaction Wheel is getting isolated or the MCS and MFS lose the communication to the data bus for over 20 control cycles. The duration of one control cycle is 500 ms. The maximum number of allowed power-cycles can be configured by ground to prevent a continuous restart loop which could lead to the degradation of the affected unit. The bus software of BIROS supports the execution of autonomous power-cycles since launch as lesson learnt from TET-1. The variation of the number of autonomous power-cycles can be used as indicator for the degradation of hardware units.

The distribution of power-cycles over the mission lifetime of TET-1 and BIROS is shown in the first and second plot of Fig. 5. It can be seen that on TET-1, the most power-cycles were executed on the IMUs. A growing accumulation can be seen on IMU-2 after the failure of IMU-1 in 2019 with two to four power-cycles per day. In order to compensate the increasing number of power-cycles, the maximum allowed number of power-cycles was modified from the default value of five to seven. In 2021 and 2022, when IMU-2 was only working spontaneously, the number of autonomous power-cycles varied between zero and seven. Compared to the IMUs, only a few power-cycles were executed on the reaction wheels. On BIROS, the most power-cycles were executed on one of the reaction wheels with up to two per day. Only on very rare occasions, a power cycle was reported on one of the IMUs.

A correlation between autonomous power cycles and space weather anomalies was performed based on the number of sunspots which is an indicator for the general Sun activity and shown in the third plot of Fig. 5. The first half of the TET-1 mission was conducted during solar cycle 24 with a relatively high number of sunspots compared to the later part of the mission, which took place in a solar low between solar cycle 24 and 25. In addition to the sunspots, solar proton events with a minimum integral flux of 10 pfu ($\text{pfu} = 1 \text{ proton cm}^{-2} \text{ sr}^{-1} \text{ s}^{-1}$) at proton energies above 10 MeV are marked [11] which can cause single event effects in the electronics of satellite components. No significant correlation between space weather events and number of power-cycles could be detected although a connection between the rising solar activity of solar cycle 25 and the further degradation of IMU-2 in 2021 and 2022 cannot be excluded. To determine the impact of geomagnetic storms caused by the solar winds, the Ap index representing the daily average level for geomagnetic activity as well as the G scale (Geomagnetic Storm Scale) as defined by the National Oceanic and Atmospheric Administration (NOAA) is displayed in the fourth plot of Fig. 5 [12]. Due to the

generally low level of geomagnetic activity during the lifetime of TET-1 and BIROS, no further analysis was performed.

The geographical location of all executed autonomous power-cycles over the mission duration as well as the total strength of the geomantic field is shown in Fig. 6. It can be seen that an accumulation around the South Atlantic Anomaly (SAA) exists due to the relatively weak local magnetic field and therefore higher exposure of the satellite to solar radiation and particles. Approximately 48% of all executed autonomous power-cycles occurred in the area of the SAA. Furthermore, a total of 31 % were located above latitudes of 60°N or below latitudes of 60°S. Only a low number of power-cycles were performed during other regions with a low latitude. No significant difference could be detected in the geographical location of power-cycles between TET-1 and BIROS and the affected AOCs unit.

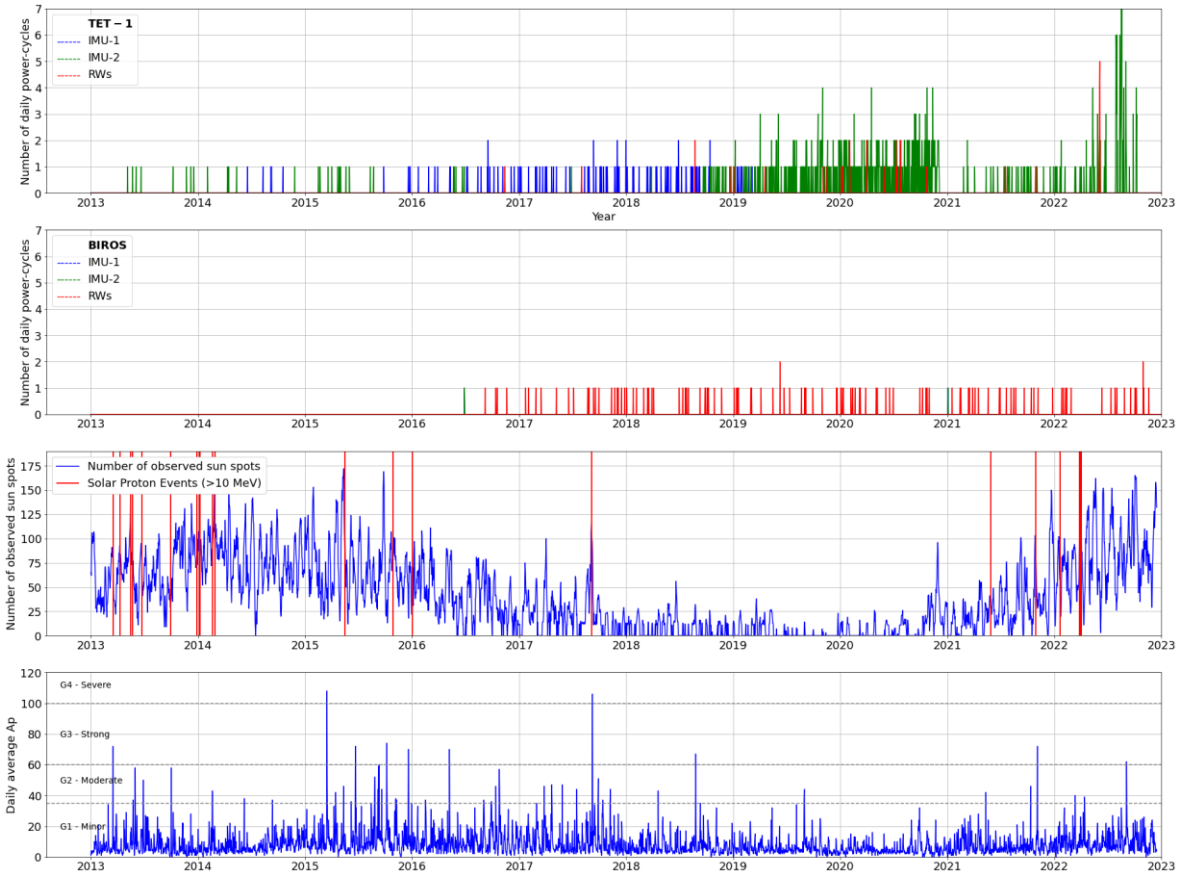


Fig. 5. Number of autonomous power-cycles executed on TET-1 (first plot) and BIROS (second plot) over time. The colours indicate the AOCs unit which performed the power-cycle. The third plot shows the number of sunspots and the time of all solar proton events with an integral proton flux of 10 pfu ($\text{pfu} = 1 \text{ proton cm}^{-2} \text{ sr}^{-1} \text{ s}^{-1}$) at energies $>10 \text{ MeV}$ [11]. The fourth plot shows the daily average Ap index with the NOAA scale for geomagnetic storms [12].

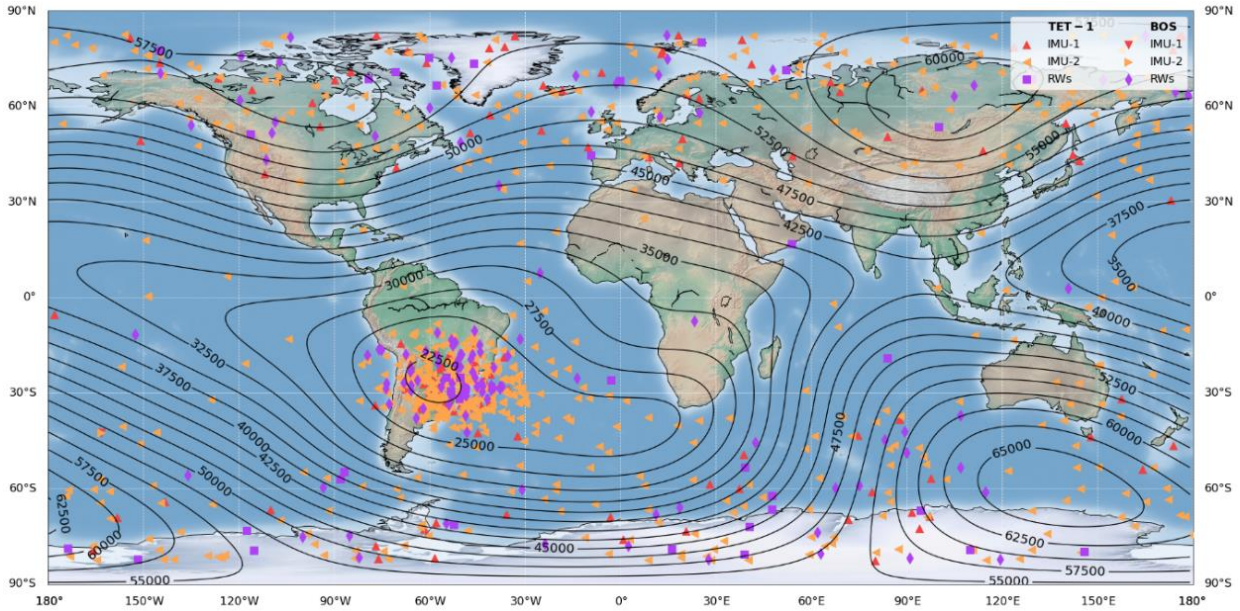


Fig. 6. Geographical location of autonomous power-cycles executed on TET-1 and BIROS with respect to the total strength of the geomagnetic field in nanotesla based on the World Magnetic Model 2020 of the NOAA [13].

6. GPS Performance

For orbit determination on-board and on-ground as well as for time synchronization, both satellites were equipped with two cold redundant miniature Phoenix GPS modules developed by DLR. The modules consume approximately 1W of electrical power and use the single frequency GPS L1 Coarse Acquisition (C/A) code with 12 fully independent tracking channels [14]. On TET-1, the receiver antennas were mounted in +x and -x direction due to design constraints. On BIROS, the antennas were both mounted in -z direction facing away from Earth during Sun phase. As shown in Table 2, the GPS is actively powered in all Fine Pointing Modes and not used in the SFM and AAM.

Over the complete lifetime of TET-1, the availability of the GPS was 76 % for receiver 1 and 66 % for receiver 2. The performance of the GPS on TET-1 expressed as percentage of valid GPS solution per day is shown in Fig. 7. Despite the overall high availability, spikes to very low values can be seen which were mainly caused by S/C anomalies and the related GPS switch off. A reduction in performance can be seen in the beginning of 2020 with an overall decrease of the GPS availability down to 34 % and a further reduction to values below 20% in February 2021. Based on this, the input for the on-ground orbit determination at GSOC was switched to NORAD TLE files instead of GPS data. A temporary switch to the redundant GPS receiver 2 was performed several times during the mission for performance comparison. Due to a high number of required restarts executed by ground operators, the GPS was permanently switched off in September 2021. In October 2022, the GPS was again switched on for closer orbit monitoring at lower altitudes. The last PVT solution received on-ground before the re-entry of the satellite was on the 16th of November at an altitude of 212 km.

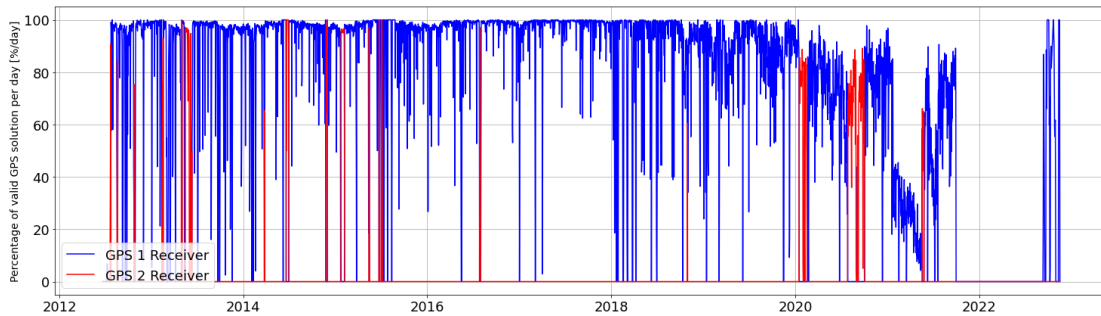


Fig. 7 TET-1: GPS availability over lifetime expressed as percentage of valid GPS solution per day

Over the complete lifetime of BIROS until December 2022, the availability of the GPS was 89 % for receiver 1 and 92 % for receiver 2. The performance of the GPS on BIROS expressed as percentage of valid GPS solution per day is shown in Fig. 8. The significantly higher performance compared to the GPS of TET-1 is caused by the different mounting of the receivers and the implementation of an on-board GPS autorestart function. In case a navigation fix is lost for 30 minutes, an autonomous warm start of the GPS is performed. To prevent the continuous execution of warm restart due to a persistent problem, a timeout is active that inhibits a follow-up restart for 30 minutes. Compared to other satellite missions, no general performance decrease can be determined connected to the so-called flex power operation of the GPS which was temporarily active several times in the years 2017 and 2018 and is now active since 2020 causing a variation in the transmitted power of the GPS satellites [15].

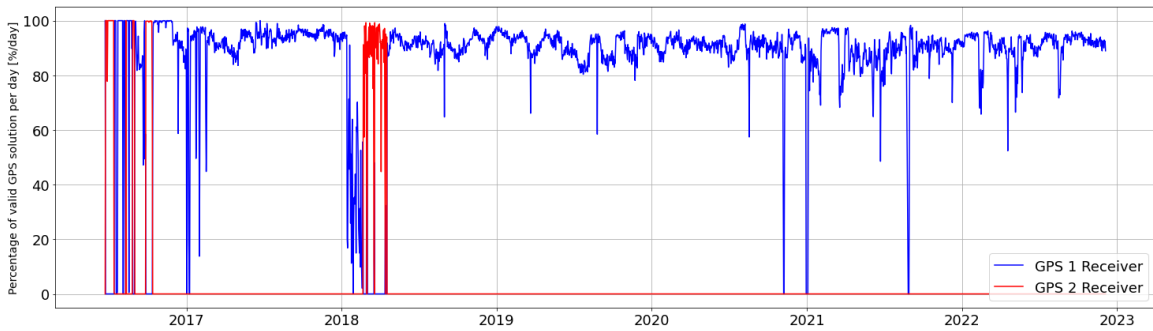


Fig. 8 BIROS: GPS availability over lifetime expressed as percentage of valid GPS solution per day

7. Star Tracker Outages

TET-1 and BIROS use two star tracker heads with a cold redundant star tracker electronics. The star tracker heads are mounted in satellite +z direction with an 35° offset to the -x and +x axes and an 7° offset in y axes as shown in . Due to the satellite design, short baffles were used which led to exclusion cones of 65° for Sun blindings and 70 – 90° for Earth blindings, depending on the illumination of the Earth’s surface. To avoid a drop from Fine Pointing Modes to Coarse Pointing Modes, the AOCS propagates the fine attitude over a configurable duration of 30 minutes which suffices to cover star tracker outages.

TET-1 was launched into a Sun-synchronous orbit with a local time of ascending node (LTAN) of 11:27 UTC. The resulting field of view of the star trackers was roughly perpendicular to the connection line Earth to Sun during activities in the SPFM and EPM reducing blinding effects to a minimum. During the time of the mission, the orbit drifted and the beta angle, defining the angle of the orbital plane with respect to the direction of the Sun, increased to values above 70° in 2018. BIROS was launched into a Sun-synchronous orbit with a LTAN of 21:30 UTC with a lower orbit drift over time. The beta angles for the orbit of TET-1 and BIROS is shown in Fig. 9.

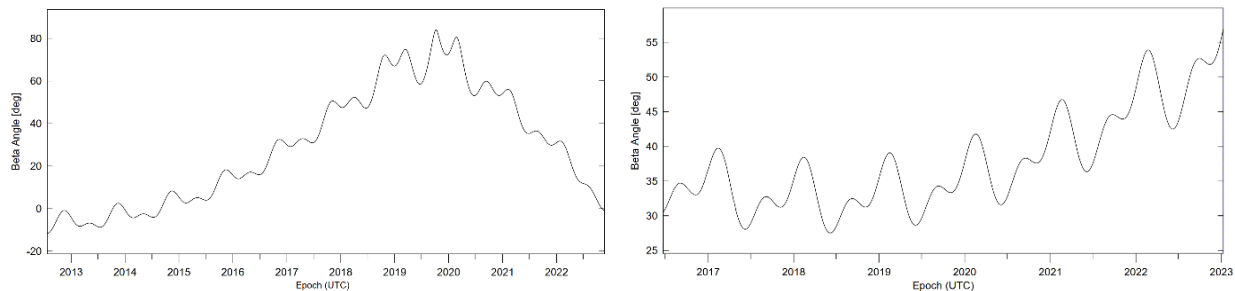


Fig. 9 Beta Angle of the TET-1 and BIROS orbit over the lifetime

The resulting availability of star tracker data for TET-1 in the modes SPFM and EPM is shown in Fig. 10. During the beginning of the mission until the end of 2014, an average of 75 % of valid data was available in SPFM and 89% of valid data in EPM. With the drift of the beta angle the blinding effects by the Sun and the Earth increased steadily. In mid of 2018, the average availability of star tracker data in the mode SPFM had decreased down to 40% and down to 0% in EPM. In November 2018, experiments were performed with additional yaw bias angles during downlinks in EPM of -90 and 90 which resulted in a significant improvement of the availability of star tracker data. For image

acquisition in EPM, an extra yaw bias of 180° was applied pointing the star trackers to the opposite direction of the Sun. After 2020, the beta angle decreased again which led to an increase of available star tracker data during SPFM comparable to values in 2015 and 2016.

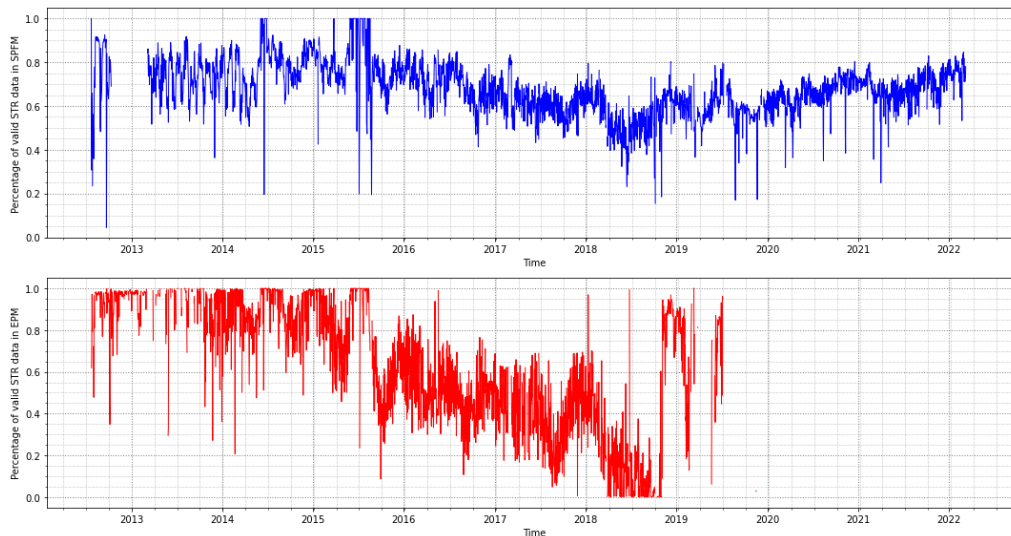


Fig. 10 TET-1: Availability of valid star tracker measurements in AOCS SPFM and EPM

With a different LTAN of the initial BIROS orbit, the availability of valid star tracker measurements after launch was lower compared to TET-1 as shown in Fig. 11. Especially during EPMs, a strong connection associated to the beta angle can be seen with a significant drop in the end of 2020 which was caused by Sun blindings. Due to the EOL operations, no further experiments with bias angles were performed to optimize the star tracker field of view.

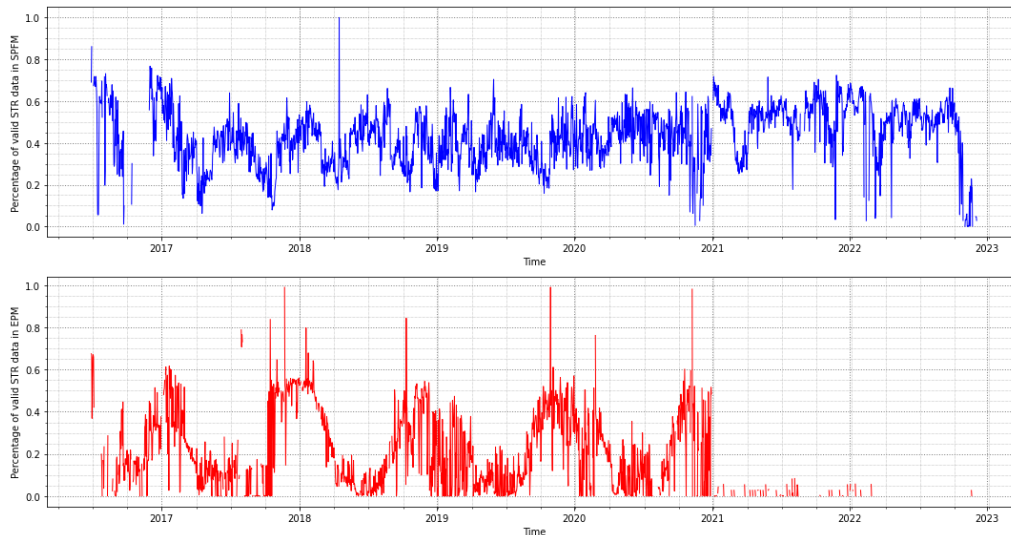


Fig. 11 BIROS: Availability of valid star tracker measurements in AOCS SPFM and EPM

In addition to the orbit dependent blinding effects, a further reduction of the star tracker performance is related to the operational temperature. This correlation can be seen during periods with additional heaters enabled on-board for payload operations. One exemplary period with heaters enabled on BIROS is shown in Fig. 12. The heaters were active for a total of 11 hours and 23 minutes increasing the temperature of the payload area by 13°C. At the same time, the temperature measured at the outer case of the star tracker heads increased from 18°C up to a maximum of 24°C, causing an outage of approximately 4 hours and 30 minutes. This led to several short transitions from SPFM to

AAM due to the lack of precise attitude data. As a result of this behaviour, and due to the extra load for the battery caused by the power consumption of the heaters, such heating periods are performed as short as possible.

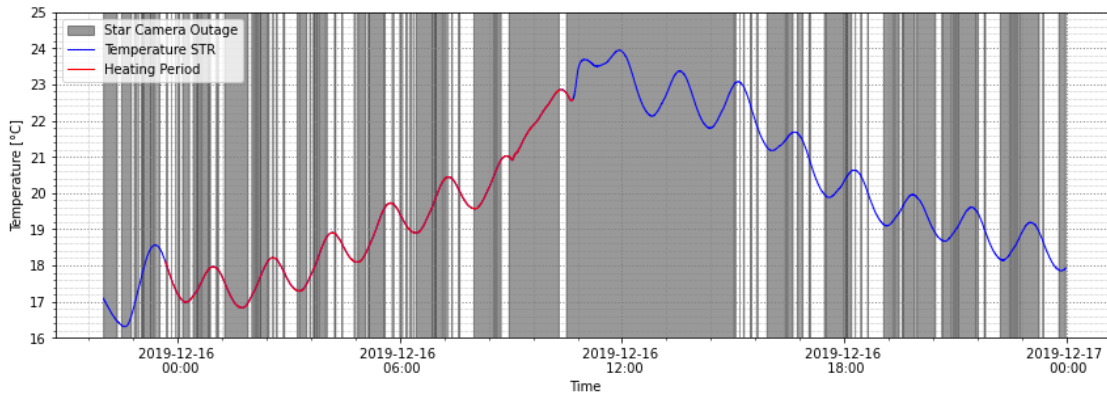


Fig. 12. BIROS: Unavailability of star tracker data due to too high temperatures

8. BEESAT-4 FlyBy Experiments with BIROS

During the launch of BIROS, the satellite was equipped with an integrated pico-satellite launcher carrying BEESAT-4 (Berlin Experimental and Educational Satellite-4), a 1U satellite developed by the Technical University of Berlin. After the successful separation of BEESAT-4 on the 9th of September 2016, it was part of the AVANTI experiment (Autonomous Vision Approach Navigation and Target Identification system) used for the demonstration of autonomous rendezvous with a passive client based on vision-based navigation in the range of 0.1 km to 10 km. The experiments were performed in the AOCS mode COM, a one axis stabilized mode around the axis of one star tracker head, which was used for the detection of BEESAT-4. Two fully automated approaches were performed in November 2016 contributing to the further development of future debris removal missions [16].

A second experiment with BEESAT-4 was the operation of the inter-satellite link, called N-Link. This modem enabled the communication between BIROS and BEESAT-4 using Ultra-High-Frequency (UHF) up to a distance of 500 km with the two UHF antennas mounted in the -z direction of BIROS. A series of N-Link experiments was performed in 2019 and 2022 during several fly-bys between both satellites near the polar regions. The goal of the experiments was the transfer of commands for an image acquisition from BIROS to BEESAT-4 and the reception of housekeeping data as well as image data from BEESAT-4 on BIROS. Since the AOCS mode COM was not available anymore at that time for supporting the continues tracking of a second object after an update of the on-board S/W, the pointing of the UHF antennas had to be approximated by using the existing AOCS modes instead.

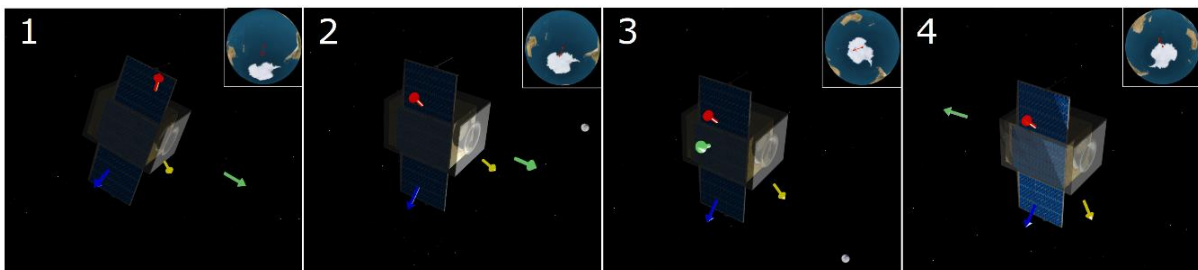


Fig. 13. Relative orientation of BIROS during the first series of flybys using the EPM over the south pole. Red arrow: flight direction, yellow arrow: Sun direction, blue arrow: direction to Earth, green arrow: direction to the BEESAT-4 satellite

During a first series of flybys, the satellite pointing was done based on one to four EPM commands per flyby modified with additional bias angles for the orientation of the UHF antenna. In-between the flybys, the AOCS was commanded back to the SPFM. The post-analysis revealed that a pointing deviation between the BIROS -z axis and the direction of BEESAT-4 was $< 90^\circ$ for the duration of the selected time slots and $< 45^\circ$ for approximately 40 % of the time. A graphical illustration of the BIROS attitude during one flyby is shown in Fig. 13.

To prolong the time of the inter-satellite link, the following series of flybys were performed using the Inertial Pointing Mode (IPM). The IPM allows a satellite pointing based on a set of commanded quaternions, representing the rotation in the S/C body axes related to the inertial True of Date (TOD) coordinate system. The commanded quaternions were calculated to express the predicted difference in position between both satellites during the flybys. The relative timing of the commands was selected to ensure that BIROS AOCS had enough time to perform the slew from the initial SPFM before the flyby and the slews between the commanded IPMs with the default slew rate of 0.5 deg/s. Depending on the varying distance between both S/Cs and the resulting required angular velocity needed to follow BEESAT-4, the number of the commanded IPMs included enough buffer to prevent the interruption of an ongoing slew. Another limitation of the experiments was the Sun offset angle relative to the solar panels. To avoid a too low discharge of the battery, the duration of slots containing one flyby had to be limited depending on their position in orbit (Sun phase vs. eclipse). A list of all performed flyby experiments can be seen in Table 4. Based on the reception report of the operations team of BEESAT-4, the flybys in 2020 were performed with further roll and pitch offsets to maximize the signal strength of the link.

Table 4. Overview of all flyby series between BIROS and BEESAT-4 in 2019 and 2020

Datum	FlyBys	Total Time [min]	Min. Distance [km]	AOCS Mode	Comment
30.05.2019	3	51	3	EPM	-z to BEESAT-4
09.08.2019	4	58	4	IPM	-z to BEESAT-4
15.12.2019	4	46	6	IPM	-z to BEESAT-4
29.05.2020	4	58	7	IPM	Not executed due to S/C problems
23.10.2020	3	49	8	IPM	-z to BEESAT-4 with -75/+60° Pitch offset
06.12.2020	5	57	7	IPM	-z to BEESAT-4 with +45° Roll offset

The angle deviation during the last performed series of flybys is plotted in Fig. 14. It can be seen that the used slots marked in grey did not always include the times with the lowest distance between both S/Cs due to the power constraint. With this commanding approach, it was possible to keep the average angular deviation at 15.6° to ensure a stable N-Link connection.

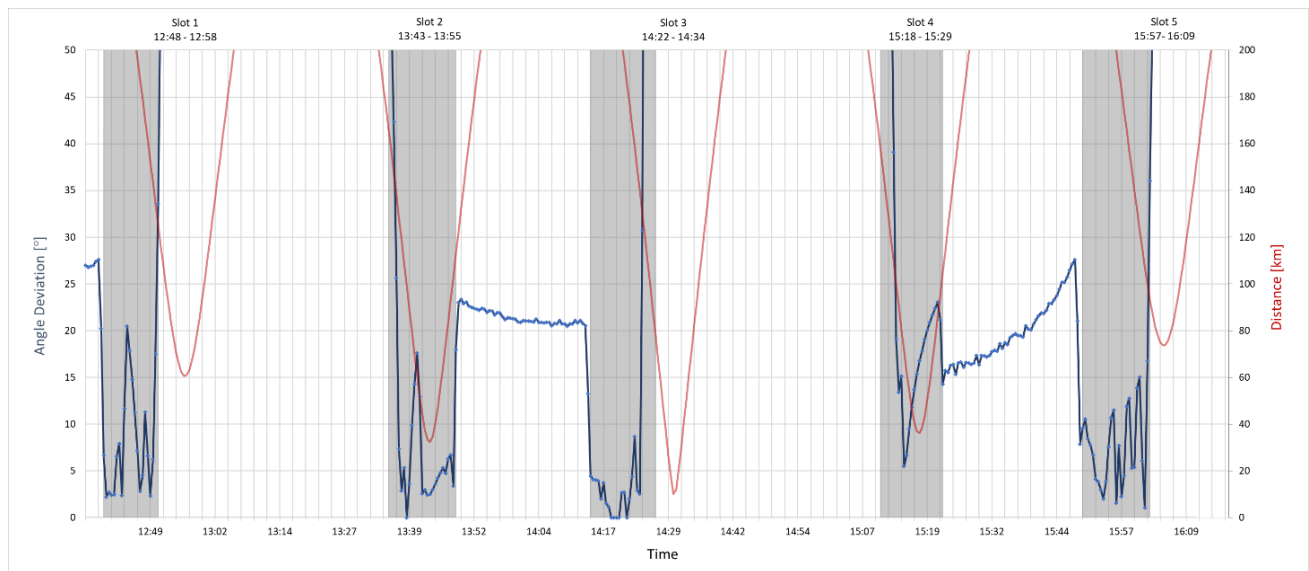


Fig. 14. Overview of angular deviation and distance between BIROS and BEESAT-4 during the last flyby experiment in December 2020. Grey areas indicate the used slots for the inter-satellite pointings.

Different options for the further improvement of the current approach are possible. A more precise prediction of the battery charge can be performed to maximize the duration of the time slots around the flybys. The selection of the commanded quaternions with the time between slews can be further optimized to approximate a smoother attitude profile. Another significant improvement can be expected by including the experimental High Torque Wheels. These

provide a higher agility with achievable angular rates of up to 10 degrees per second to support the time frames with a very low inter-satellite distance [17].

9. Conclusion and Outlook

This paper presented the experiences during the operation of the AOCS of TET-1 and BIROS during the FireBird mission and the following EOL period, and a selection of challenges that occurred. Due to the robust design and redundancy concept of the AOCS, the failure of one Inertial Measurement Unit and one Reaction Wheel was compensated without significant performance reduction. After the subsequent degradation and failure of the redundant Inertial Measurement Unit, the input of the remaining sensors was sufficient enough to ensure the successful execution of basic tasks, such as the establishment of a Sun pointing attitude for battery recharging and an Earth pointing attitude for a stable uplink of telecommands and downlink of telemetry. The result of the execution of autonomous power-cycle of AOCS hardware units was outlined and the performance of the GPS receivers and the star trackers over the years discussed. A method to establish the required attitude pointing during inter-satellite links with BIROS via UHF was presented demonstrating the flexible support of experiments by the AOCS design. With the operation of TET-1 over a time period of 10 years, valuable experiences have been collected at GSOC for upcoming long-term missions and re-entry phases of small satellites in the low Earth orbit. With the fully operational BIROS satellite in space, further experiments can be supported on a cost-effective bases and training of GSOC personal can be performed for the remaining years until the projected re-entry in 2029.

Acknowledgements

The author would like to thank the colleagues of the FireBird mission operations and flight dynamics team at GSOC for the good teamwork and pleasant work environment, and the members of the DLR Institute of Optical Sensor Systems in Berlin for the support.

References

- [1] K. Brieß, W. Bärwald, T. Gerlich, H. Jahn, F. Lura and H. Studemund, "The DLR Small Satellite Mission Bird," *Acta Astronautica*, pp. 111-120, Vol. 46 2000.
- [2] S. Föckersperger, K. Lattner, C. Kaiser, S. Eckert, S. Ritzmann, R. Axmann and M. Turk, "THE ON-ORBIT VERIFICATION MISSION TET-1," 2010.
- [3] E. Lorenz, W. Halle, C. Fischer, N. Mettig and D. Klein, "RECENT RESULTS OF THE FIREBIRD MISSION," in *37th International Symposium on Remote Sensing of Environment*, Tshwane, South Africa, 2017.
- [4] T. Terzibaschian, Space Craft User Manual BIROS-DLR_MA-002 Part 2, DLR - Institute of Optical Sensor Systems, 2015.
- [5] H. Adirim, M. Kreil, M. Kron, A. Mitrofanow, W. Halle, M. Lieder, W. Bärwald, S. Babben and T. Terzibaschian, "Innovative Modular Propulsion Systems for Small Satellites," in *Proc. 10th IAA Symp. on Small Satellites for Earth Observation*, Berlin, Germany, 2015.
- [6] S. Löw, J. Herman and D. Schulze, "Modes and More - Finding the Right Attitude for TET-1," in *Space Ops 2012*, Stockholm, Sweden, 2012.
- [7] A. Tewari, *Advanced Control of Aircraft, Spacecraft and Rockets*, Wiley, 2011.
- [8] L. Markley and J. L. Crassidis, *Fundamentals of Spacecraft Attitude Determination and Control*, Springer Science and Business Media, 2014.
- [9] K. A. Larson, K. M. McMalmnt, C. A. Perterson and S. E. Ross, "Kepler Mission Operations Response to Wheel Anomalies," in *SpaceOps 2014*, Pasadena, CA, USA, 2014.
- [10] M. D. Rayman and R. A. Mase, "Dawn's operations in cruise from Vesta to Ceres," *Acta Astronautica*, pp. 113-118, October-November 2014.
- [11] "Space Weather Prediction Center - National Oceanic and Atmospheric Administration, NOAA Space Weather SEP list," [Online]. Available: <ftp://ftp.swpc.noaa.gov/pub/indices/SPE.txt>. [Accessed 2022 12 15].
- [12] "CelesTrak - Earth Orientation Parameters and Space Weather Data for Flight Operations," [Online]. Available: <https://celestrak.org/SpaceData/>. [Accessed 15 12 2022].

- [13] "World Magnetic Model 2020. NOAA National Centers for Environmental Information," NCEI Geomagnetic Modeling Team and British Geological Survey, 2019. [Online]. Available: <https://www.ngdc.noaa.gov/geomag/WMM/soft.shtml>. [Accessed 15 12 2022].
- [14] O. Montenbruck and C. Renaudie, "Phoenix Miniature GPS Receiver - Phoenix-S/-XNS Performance Validation," 05 April 2007. [Online]. Available: https://www.dlr.de/rb/en/desktopdefault.aspx/tabid-10749/10533_read-23353/. [Accessed 16 12 2022].
- [15] P. Steigenberger, S. Thöler and O. Montenbruck, "Flex power on GPS Block IIR-M and IIF," *GPS Solutions*, Vol. 23 2019.
- [16] Ardaens, Jean-Sébastien; Gaias, Gabriella; Schultz, Christian, "THE AVANTI EXPERIMENT: FLIGHT RESULTS," in *GNC 2017: 10th International ESA Conference on Guidance, Navigation & Control*, Salzburg, Austria, 2017.
- [17] T. Terzibaschian, R. Christian, W. Bärwald, A. Kotz, C. Schultz, X. Amigues, A. Choinowski and W. Halle, "71st International Astronautical Congress (IAC)," in *High Torque Wheels for agile Satellite Maneuvers - in Orbit Experiences and future Steps with*, Online, 2020.